Plant Molecular Biology (2022) 110:445–454
https://doi.org/10.1007/s11103-022-01246-z

REVIEW

A scheme for C_4 evolution derived from a comparative analysis of the closely related C_3, C_3–C_4 intermediate, C_4-like, and C_4 species in the genus *Flaveria*

Yuri N. Munekage[1] · **Yukimi Y. Taniguchi**[1]

Received: 18 November 2021 / Accepted: 21 January 2022 / Published online: 4 February 2022

Abstract

Key message **A comparative analysis of the genus *Flaveria* showed a C_4 evolutionary process in which the anatomical and metabolic features of C_4 photosynthesis were gradually acquired through C_3–C_4 intermediate stages.**

Abstract C_4 photosynthesis has been acquired in multiple lineages of angiosperms during evolution to suppress photorespiration. Crops that perform C_4 photosynthesis exhibit high rates of CO_2 assimilation and high grain production even under high-temperature in semiarid environments; therefore, engineering C_4 photosynthesis in C_3 plants is of great importance in the application field. The genus *Flaveria* contains a large number of C_3, C_3–C_4 intermediate, C_4-like, and C_4 species, making it a good model genus to study the evolution of C_4 photosynthesis, and these studies indicate the direction for C_4 engineering. C_4 photosynthesis was acquired gradually through the C_3–C_4 intermediate stage. First, a two-celled C_2 cycle called C_2 photosynthesis was acquired by localizing glycine decarboxylase activity in the mitochondria of bundle sheath cells. With the development of two-cell metabolism, anatomical features also changed. Next, the replacement of the two-celled C_2 cycle by the two-celled C_4 cycle was induced by the acquisition of cell-selective expression in addition to the upregulation of enzymes in the C_4 cycle during the C_3–C_4 intermediate stage. This was supported by an increase in cyclic electron transport activity in response to an increase in the ATP/NADPH demand for metabolism. Suppression of the C_3 cycle in mesophyll cells was induced after the functional establishment of the C_4 cycle, and optimization of electron transport by suppressing the activity of photosystem II also occurred during the final phase of C_4 evolution.

Keywords *Flaveria* · C_4 evolution · C_4 photosynthesis · Photorespiration · C_3–C_4 intermediate · Cyclic electron transport

Introduction

Global warming in recent years has caused extreme weather events such as severe droughts and heat waves, which affect ecosystems and vegetation and reduce crop production. Under drought, plants close their stomata. This regulation is important to prevent water loss in plants but also limits the entry of CO_2. The resulting decrease in intracellular CO_2 enhances the oxygenase activity of ribulose-1,5-bisphosphate carboxylase-oxygenase (RuBisCO) in chloroplasts. High temperature also enhances RuBisCO oxygenase activity by decreasing the RuBisCO specificity to CO_2 relative to O_2 in addition to decreasing the ratio of dissolved O_2 to dissolved CO_2 in the chloroplast (Jordan and Ogren 1984; Long 1991). At the current atmospheric CO_2 concentration of approximately 400 ppm, photorespiration occurs at a rate of 25% of photosynthesis at 30–35 °C and over 40% of photosynthesis at 35–40 °C (Sage et al. 2012). C_4 plants are able to suppress photorespiration by concentrating CO_2 at RuBisCO sites; therefore, they have a great advantage for survival in hot and semiarid environments compared with C_3 plants. Metabolic pathways have been extensively studied, and attempts have been made to introduce the C_4 cycle into C_3 plants. However, the engineering of C_4 photosynthesis is still a work in progress, and the entire system that coordinates C_4 photosynthesis needs to be clarified. (Ermakova et al. 2021; Lin et al. 2020; Taniguchi et al. 2008). Meanwhile, phylogenetic studies of various genera, phenotypic comparisons, and a recent comprehensive transcriptome have demonstrated that C_4 evolution occurred

✉ Yuri N. Munekage
munekage@kwansei.ac.jp

[1] School of Science and Technology, Kwansei Gakuin University, 2-1 Gakuen, Sanda, Hyogo 669-1337, Japan

gradually through C_3–C_4 intermediate stages (Lauterbach et al. 2017; Lyu et al. 2015; Mallmann et al. 2014; Williams et al. 2013). C_4 evolution has occurred more than 66 times in angiosperms, indicating that there may be a common system in C_3 plants that leads to C_4 evolution (Sage et al. 2012). The genus *Flaveria* in the family Asteraceae evolved relatively recently three hundred million years ago and contains a variety of species, including C_3, C_3–C_4 intermediate, C_4-like and C_4 species, making it a good model genus for studying the evolution of C_4 photosynthesis (Christin et al. 2011; Ku et al. 1991; Powell 1978). Biochemical and biophysical evidence of *Flaveria* is accumulating, and we recently published draft genome sequences of C_3 *Flaveria robusta*, C_3–C_4 intermediate *Flaveria floridana*, C_4-like *Flaveria brownii* and C_4 *Flaveria bidentis* (Taniguchi et al. 2021). By tracing the genomic changes associated with changes in photosynthesis, we hope to clarify the molecular mechanisms underlying C_4 evolution and to provide missing information for engineering C_4 photosynthesis in C_3 plants. In this review, we present the characteristics of C_3, C_3–C_4 intermediate, C_4-like, and C_4 *Flaveria* species and propose a scheme for C_4 evolution derived from studies of *Flaveria*.

During the 3 million years of C_4 evolution in the genus *Flaveria*, genome size, not the number of encoded genes, has changed enormously

Twenty-three species are recognized in the genus *Flaveria,* and most of these species were reported to be diploid (n = 18), except for *F. pringlei* (n = 36), which is an allopolyploid of *F. pringlei* and *F. angustifolia* (Lyu et al. 2015; McKown et al. 2005; Powell 1978). Figure 1 shows the phylogenetic tree of 20 species in the genus *Flaveria* and the genome sizes of selected species among them (McKown et al. 2005; Taniguchi et al. 2021). Phylogenetic studies showed that C_3–C_4 intermediate species appeared between 3.6 and 3.1 million years ago, except for *F. sonorensis,* which appeared 2.8 million years ago (Christin et al. 2011; McKown et al. 2005). The transition from C_3–C_4 intermediates to C_4-like traits has occurred twice in the genus *Flaveria* and is estimated to have occurred between 1.8 and 1.3 million years ago in clade A and after 0.4 million years ago in clade B (Christin et al. 2011; McKown et al. 2005). The transition from the C_4-like trait to the C_4 trait occurred only in clade A, which is estimated to have occurred after 1 million years ago. They are mostly distributed in tropical and subtropical regions, such as Mexico, the Gulf Coast of the United States, and the West Indies (McKown et al. 2005). Geographic studies have suggested that the transition from C_3 to C_3–C_4 intermediates, C_4-like, and C_4 photosynthesis in the genus *Flaveria* may have been triggered by high temperatures, frequent droughts, and increased salinity, as suggested by the evolution of many other C_4 species (Edwards et al. 2010; McKown et al. 2005; Sage et al. 2012). Interestingly, although the genome sizes of these *Flaveria* species vary widely, indicating that their genomes have changed significantly during evolution (Fig. 1), the number of protein-coding genes predicted by mapping mRNAs to whole-genome draft data was not affected (Taniguchi et al. 2021). The genome size of the basal Group C_3 *F. robusta* is the smallest at 0.49 Gb, the genome size of C_4 *F. bidentis* in clade A is twice that at 1.01 Gb, and the genome size of C_3–C_4 intermediate *F. floridana* and C_4-like *F. brownii* in clade B is 1.39 Gb and 1.58 Gb, respectively, but all four species contain approximately 40,000 protein-coding genes (Taniguchi et al. 2021). These species have almost the same number of gene families of C_4 cycle enzymes, and the expression of one of the genes was upregulated and acquired a cell-specific expression pattern during C_4 evolution (Taniguchi et al. 2021). These results suggest that basal group *Flaveria* species have the potential to evolve to C_4 and/or are already in the preliminary stages of C_4 evolution, and changes in *cis*-elements and/or trans-factors that control gene expression may have led to actual C_4 evolution.

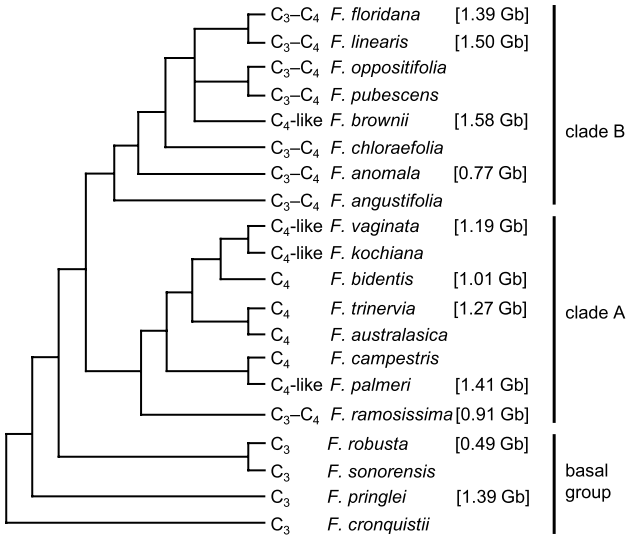

Fig. 1 Phylogenetic tree of 20 species in the genus *Flaveria* and genome sizes of selected species among them. Relative branch points in the phylogenetic tree and clade classification of species were based on McKown et al. (2005). Genome size of *Flaveria* species was based on Taniguchi et al. (2021)

Alteration of leaf anatomy supporting a two-celled metabolic cycle during the transition from C_3 to C_4 photosynthesis

To compare plant phenotypes and gene expression, plants were grown in a growth chamber with a light intensity of 200–300 µmol photons m^{-2} s^{-1} at 24 °C in our study (Munekage et al. 2010; Nakamura et al. 2013; Taniguchi

et al. 2021). Under this condition, *Flaveria* C_3 and C_4 species have typical CO_2 concentration points (Γ) and O_2 inhibition of photosynthesis compared with other C_3 and C_4 plants, respectively, and C_3–C_4 intermediate and C_4-like species have values between C_3 and C_4 species (Table 1) (Jordan and Ogren 1984; Ku et al. 1991). Since flowering in the genus *Flaveria* is induced under short-day conditions, for morphological analysis, plants were grown under long-day conditions to prevent early flowering (Fig. 2). C_3 *F. pringlei*, C_3 *F. robusta*, C_3–C_4 F. *floridana*, C_4 *F. bidentis* and C_4 *F. trinervia* have broad leaves (Fig. 2A, C, E, M and O), whereas C_3–C_4 *F. ramosissima*, C_4-like *F. brownii* and C_4-like *F. palmeri* have narrow leaves (Fig. 2G, I and K). The size and shape of leaves are genetically or conditionally determined as a result of adaptation to the environment. For example, plants form smaller leaf surface areas to minimize water loss in dry environments, but leaf size and shape are not related to the type of photosynthesis in the genus *Flaveria* (Fig. 2). On the other hand, leaf anatomy is closely related to the type of photosynthesis (Fig. 2).

Common anatomical features that have changed in association with the evolution to C_4 photosynthesis include (i) a decrease in intervascular distance correlated with a decrease in the number of mesophyll cells located between bundle sheath cells, (ii) an enlargement of the volume of bundle sheath cells relative to the volume of mesophyll cells, (iii) an increase in the number of mitochondria and chloroplasts oriented centripetally or centrifugally within bundle sheath cells, and (iv) radial patterning of a single mesophyll cell layer surrounding bundle sheath cells (Lundgren et al. 2014; Sage et al. 2012). These features are important for the two-celled metabolism of C_4 photosynthesis. The enlargement of bundle sheath cells and the increase in the number of organelles in these cells are necessary to support the metabolic activities of bundle sheath cells. The reduced intervascular distance and the radial patterning of a single mesophyll cell layer that surrounds the bundle sheath cells also contribute to the rapid exchange of metabolites between mesophyll and bundle sheath cells. These C_4-type features, often collectively referred to as Kranz anatomy, must be regulated by different molecular mechanisms, and it is likely that they were obtained in a stepwise fashion through intermediate stages.

(i) In the genus *Flaveria*, intervascular distance correlates well with the degree of C_4 evolution: the C_3 basal species have longer intervascular distances and four or more mesophyll cells between vascular bundles, whereas the C_3–C_4 intermediate species have reduced intervascular distances, and the C_4-like and C_4 species have more pronounced reductions in intervascular distances and approximately two mesophyll cells between vascular bundles (Fig. 2) (McKown and Dengler 2007). This trait is attributed to the enhanced development of minor veins (McKown and Dengler 2009). Auxin signaling appears to be an important factor controlling vein

Table 1 Characterization of C_3, C_3–C_4 intermediate, C_4-like and C_4 species in the genus *Flaveria*

Species	*F. pringlei*	*F. robusta*	*F. floridana*	*F. ramosissima*	*F. brownii*	*F. palmeri*	*F. bidentis*	*F. trinervia*
Type	C_3	C_3	C_3–C_4	C_3–C_4	C_4-like	C_4-like	C_4	C_4
Γ (μmol CO_2 mol^{-1})	50 ± 3	47.6 ± 0.4	16 ± 1	24 ± 1	11 ± 3	12 ± 1	3.3 ± 1.4	2.8 ± 1.0
O_2 inhibition (%)	48 ± 1	55 ± 3	44 ± 3	40 ± 2	26 ± 2	7.4 ± 1.5	5.0 ± 0.7	3.4 ± 0.3
Relative expression of C_4 enzymes (PEPC, PPDK, ME1)	< 0.03	< 0.03	0.1, 0.3, 0.5	0.2, 0.3, 0.6	0.3, 0.6, 1.6	≒1	≒1	≒1
cell selective distribution of C_4 enzymes	n.d	n.d	No	Weak	Strong	Very strong	Very strong	Very strong
RuBisCO expression in M cell	Strong	Strong	Strong	Strong	Weak	Weak	No	No
CET activity $P700^+$ $t_{3/4}$ (s)	0.48 ± 0.06	0.7 ± 0.1	1.3 ± 0.4	3.3 ± 0.7	3.3 ± 0.8	8.6 ± 0.6	10.6 ± 0.6	9.1 ± 0.6
Grana index of BS chloroplasts (%)	n.d	n.d	n.d	63	50	16	15	19

CO_2 compensation point (Γ), O_2 inhibition of photosynthetic activity (O_2 inhibition), relative expression and cell selective distribution of C_4 enzymes, RuBisCO expression in mesophyll (M) cells, cyclic electron transport (CET) activity and grana index in bundle sheath (BS) chloroplasts of selected *Flaveria* species are shown. The CO_2 compensation point and O_2 inhibition were measured at 25 °C and 50% humidity using an LI-6400 portable photosynthesis system equipped with a blue–red light-emitting diode (LED) light source, LI-6400-40 (LI-COR, Inc., Lincoln, NE, USA). CO_2 compensation points were determined from an extrapolation point of zero on the regression line, CO_2 response curves between 30 and 400 μmol mol^{-1} under constant irradiance (1000 μmol photons m^{-2} s^{-1}). O_2 inhibition of photosynthetic activity was calculated from the difference in photosynthesis at 21% O_2 and 2% O_2 under conditions of 150 μmol mol^{-1} intercellular CO_2 concentration (Ci) and 1500 μmol photons m^{-2} s^{-1}. Data represent mean ± SD for n = 3–4. The relative expression and cell selective distribution of C_4 enzymes were based on Taniguch et al. (2021). CET activity estimated by P700 oxidation kinetics ($t_{3/4}$, the time required to achieve 3/4 of the steady level of $P700^+$) was calculated from data on Nakamura et al. (2013). P700 oxidation kinetics for *F. floridana* were determined with the same measurement conditions as that in Nakamura et al. (2013). Data represent mean ± SD for n = 3–5. Grana index (length of the appressed thylakoid membrane as a percentage of the total thylakoid membrane) of BS chloroplasts were based on Nakamura et al. (2013). All data were measured on plants grown under the same growth conditions at 24 °C and a light intensity of 200–300 μmol photons m^{-2} s^{-1}. n.d. indicates not determined

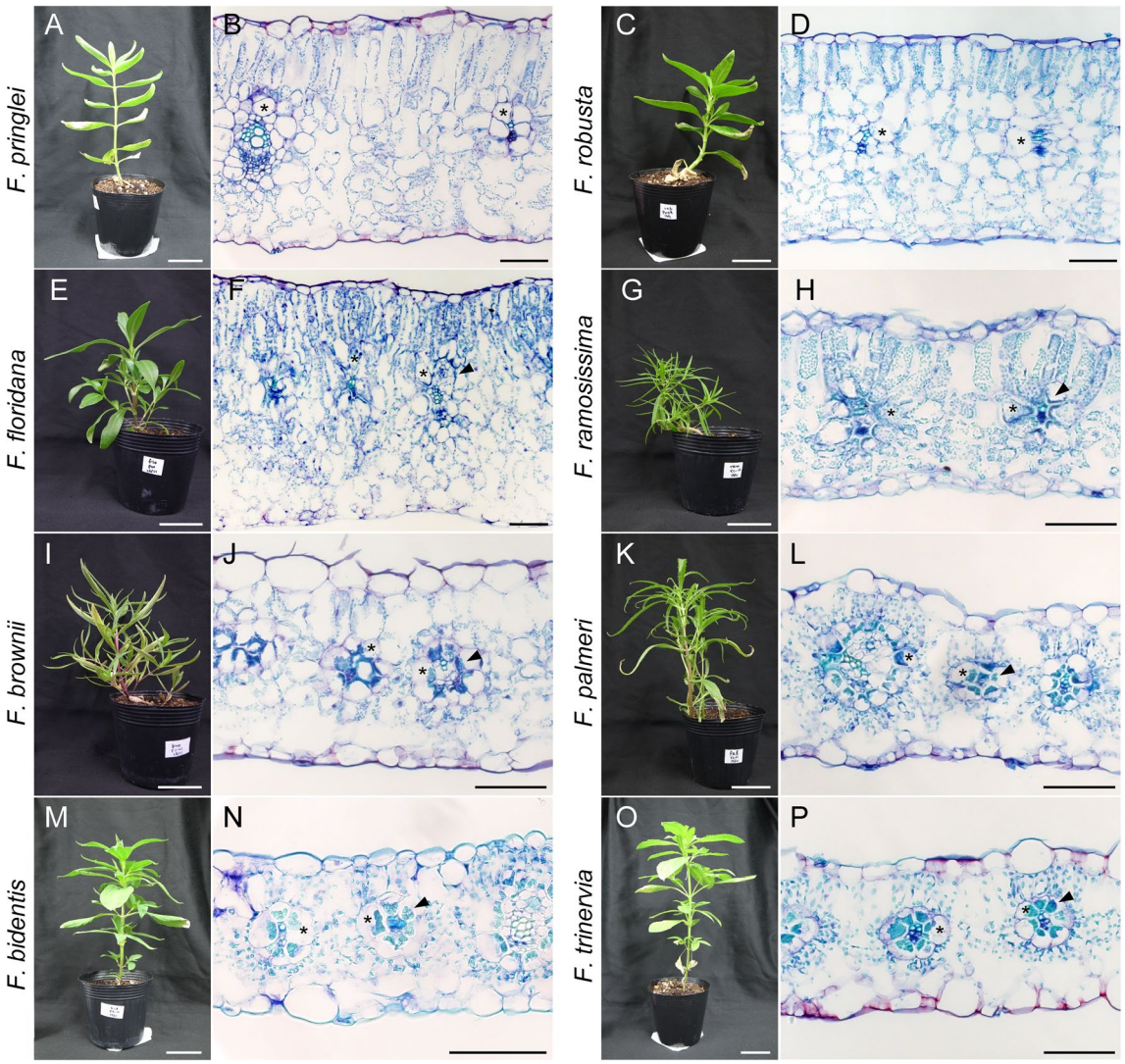

Fig. 2 Visible phenotype and leaf cross sections of *F. pringlei* (**A**, **B**), *F. robusta* (**C**, **D**) classified as a C_3 species, *F. floridana* (**E**, **F**) and *F. ramosissima* (**G**, **H**) classified as C_3–C_4 intermediate species, *F. brownii* (**I**, **J**) and *F. palmeri* (**K**, **L**) classified as C_4-like species, and *F. bidentis* (**M**, **N**) and *F. trinervia* (**O**, **P**) classified as C_4 species grown for 8 weeks in a growth chamber at a light intensity of 200–300 µmol photons m^{-2} s^{-1} with a 16 h light–8 h dark photoperiod at 24 °C. Leaf cross sections were prepared using fully expanded leaves as described in Nakamura et al. (2013). Scale bars indicate 5 cm for the picture of the plants (**A**, **C**, **E**, **G**, **I**, **K**, **M**, **O**) and 100 µm for the leaf cross section (**B**, **D**, **F**, **H**, **J**, **L**, **N**, **P**). Asterisks indicate examples of bundle sheath cells. Arrowhead indicate examples of chloroplasts in the centripetal position of bundle sheath cells

density because vein differentiation is induced by auxin maxima that are directed by PIN-FORMED auxin efflux carriers and their regulators (Linh et al. 2018; Sedelnikova et al. 2018). Although it was shown that auxin biosynthesis and the expression of related genes are higher in C_4 species (Huang et al. 2017), the mechanisms underlying the initiation of minor vein and C_4-type vein patterning have not been elucidated.

(ii) In terms of parameters for bundle sheath cell enlargement, the volume of the bundle sheath cells do not differ between C_3 and C_4 *Flaveria* species, but the relative proportion of mesophyll to bundle sheath tissue area in mature leaves is well correlated with the type of photosynthesis (McKown and Dengler 2007). The C_3–C_4 intermediate species have a ratio of mesophyll to bundle sheath tissue area between C_3 and C_4 species, while the C_4-like species have a ratio of mesophyll to bundle sheath tissue area close to C_4 species (McKown and Dengler 2007). This is thought to be due to the early cessation of proliferation and elongation of mesophyll cells during leaf expansion, resulting in a decrease in the number and volume of mesophyll cells (McKown and Dengler 2009).

(iii) The number of mitochondria and chloroplasts in the bundle sheath cells is significantly higher in C_3–C_4

intermediate species, and this phenotype is closely related to the development of a photorespiration-dependent CO_2 concentration system (Sage et al. 2014; Voznesenskaya et al. 2017; Yorimitsu et al. 2019). C_3 photosynthesis occurs within the mesophyll cell, and the bundle sheath cells do not contribute much to starch synthesis, but in C_3–C_4 intermediate species, photorespiration-dependent CO_2 concentration using mesophyll and bundle sheath cells (called C_2 photosynthesis) occurs, and starch synthesis occurs in both cells (Bauwe 2011). In the C_3–C_4 intermediate species, most of the activity of glycine decarboxylase (GDC) is lost in mitochondria of mesophyll cells; therefore, glycine is transported to bundle sheath cells and converted to serine by GDC in mitochondria of bundle sheath cells (Fig. 3A). A large proportion of chloroplasts were found to accumulate in the centripetal position of bundle sheath cells together with mitochondria in *Flaveria* C_3–C_4 intermediate species (Fig. 2F and H) (Sage et al. 2013). These two-celled C_2 cycle and organelle arrangements contribute significantly to the recapture of CO_2 released from photorespiration by elevating the CO_2 level at a site of RuBisCO in bundle sheath chloroplasts. Since C_3 *F. pringlei* and C_3 *F. robusta* were found to have more chloroplasts and mitochondria in bundle sheath cells than C_3 *F. cronquistii* and other closely related C_3 species, and GDC expression was higher in bundle sheath cells than in mesophyll cells, these species have been classified as proto-Kranz C_3 species (Sage et al. 2013, 2014). The C_4-like and C_4 species have enlarged chloroplasts located at the centripetal position in the bundle sheath cells (Fig. 2J, L, N and P), but the number of chloroplasts in these species has

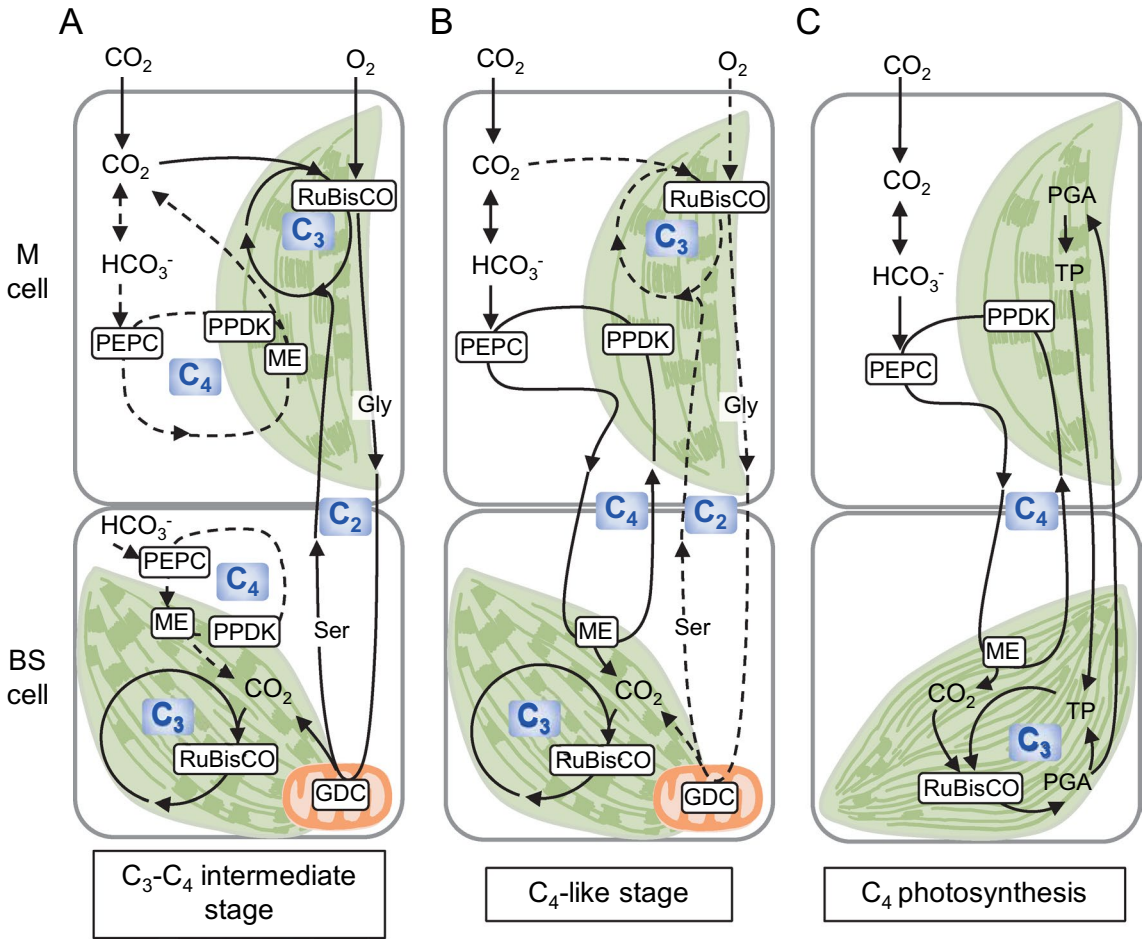

Fig. 3 Schematic representation of the metabolic pathways of the C_3–C_4 intermediate stage, C_4-like stage and C_4 photosynthesis. In the C_3–C_4 intermediate stage, noncell-specific expression of C_4 enzymes is induced in the background of C_2 photosynthesis, where glycine produced by photorespiration in mesophyll cells is shuttled to BS cells and decarboxylated by glycine decarboxylase localized in mitochondria of bundle sheath cells (**A**). In the C_4-like stage, the two-celled C_4 cycle is strongly promoted by cell-specific regulation of C_4 enzyme expression, and C_2 photosynthesis activity is reduced by suppression of RuBisCO expression in mesophyll cells (**B**). C_4 photosynthesis is established by completely restricting RuBisCO expression in BS cells (**C**). Chloroplasts and mitochondria are represented in green and orange, respectively. *M* mesophyll cell, *BS* bundle sheath cell, *C_3* C_3 cycle, *C_4* cycle, *C_2* C_2 photosynthesis, *RuBisCO* ribulose 1,5-bisphosphate carboxylase/oxygenase, *PEPC* phosphoenolpyruvate carboxylase, *PPDK* pyruvate orthophosphate dikinase, *ME* NADP-malic enzyme, and *GDC* glycine decarboxylase

not changed or has decreased except for *F. brownii,* which has a large number of small chloroplasts in bundle sheath cells (Araus et al. 1990; Brown and Hattersley 1989; Sage et al. 2014). Maize GOLDEN2-like transcription factors were shown to promote the development of bundle sheath chloroplasts in rice (Wang et al. 2017). In rice, two genes encoding GOLDEN2-like, *OsGLK1* and *OsGLK2*, were shown to be redundantly involved in chloroplast development (Rossini et al. 2001; Wang et al. 2013). On the other hand, in maize, *ZmG2*, which is related to *OsGLK2*, was preferentially expressed in bundle sheath cells, and was suggested to function in chloroplast development in these cells (Hall et al. 1998; Rossini et al. 2001). However, the mechanism that determines chloroplast enlargement, increase, and positioning remains to be elucidated.

(iv) Radial patterning, in which a single mesophyll cell layer surrounds a bundle sheath cell layer, was observed not only in monocotyledonous C_4 species but also in eudicotyledonous C_4 species (Edwards and Voznesenskaya 2011). This patterning is partly related to the number of cell layers in immature ground tissues and the loss of cell division during leaf development. In the genus *Flaveria*, basal C_3 species have eight layers of ground tissue cells in developing leaves (McKown and Dengler 2007). Of eight cell layers, cells in the first and second layers at the adaxial side of the subepidermis differentiate into palisade cells. C_3–C_4 intermediate *F. floridana* and C_4-like *F. brownii* in clade B both have six layers of immature ground tissue cells in developing leaves (McKown and Dengler 2007), but in mature leaves, *F. floridana* has two layers of palisade cells, whereas *F. brownii* has mostly one layer of mesophyll cells, and the extra mesophyll cells not adjacent to the bundle sheath cells contain few chloroplasts (Fig. 2F and J) (Araus et al. 1990; Cheng et al. 1988). Furthermore, large intercellular spaces were observed between epidermal cells in adaxial or abaxial mesophyll cells in *F. brownii* (Fig. 2J). This implies that early cessation of proliferation and development of mesophyll cells occur during leaf expansion in C_4-like *F. brownii.* Clade A species, including C_3–C_4 intermediate *F. ramosissima*, C_4-like *F. palmeri*, C_4 *F. bidentis* and C_4 *F. trinervia,* basically exhibit five layers of ground tissue cells in developing leaf tissue, and they all form a single layer of palisade mesophyll cells (Fig. 2H, L, N and P) (McKown and Dengler 2007), suggesting that the number of ground tissue layers is genetically determined in clade A. On the other hand, in C_4-like and C_4 species in clade A, the mesophyll cells are arranged around the bundle sheath cells, and most of them are adjacent to the bundle sheath cells (Fig. 2L, N and P).

Gradual replacement of the two-celled C_2 cycle with the two-celled C_4 cycle during C_4 evolution

The C_3–C_4 intermediate species exhibit a lower CO_2 compensation point than the C_3 species due to their photorespiration-dependent CO_2 concentration mechanism (C_2 photosynthesis), but their O_2 inhibition rate is high (40–44%), close to that of the C_3 species (Table 1) (Ku et al. 1991). The lower O_2 inhibition rates found in the C_4-like species (26% in *F. brownii* and 7% in *F. palmeri*) correlated with the amount of RuBisCO expression remaining in the mesophyll cell (Table 1) (Ku et al. 1991; Taniguchi et al. 2021).

The first step of C_4 evolution was the gain of C_2 photosynthesis that occurred in the transition from the C_3 to C_3–C_4 intermediate stage, which can be explained by a single event, the localization of GDC activity to the mitochondria of bundle sheath cells, as described above. C_2 photosynthesis is important under high-temperature conditions when the activity of RuBisCO oxygenase is enhanced and was suggested to have bridged the evolution of C_3 to C_4 photosynthesis (Bauwe 2011; Sage et al. 2018). GDC is composed of four proteins, P-, L-, T-, and H-protein, which catalyze the conversion of glycine to serine through a multistep enzymatic system. In the multistep reaction, the P-protein functions as the actual decarboxylation unit. Suppression of GDC P-protein in mitochondria of mesophyll cells was found in C_3–C_4 intermediate species in a number of genera, including *Steinchisma*, *Moricandia*, *Mollugo*, *Flaveria* and *Heliotropium* (Bauwe 2011; Sage et al. 2014). Studies in the genus *Flaveria* have provided an example of how bundle sheath cell-specific expression of P-protein in GDCs was acquired (Schulze et al. 2013, 2016). In *Flaveria*, the P-protein of GDC is encoded by three genes, *GLDPA*, *GLDPB* and *GLDPC*. While GLDPA and GLDPB were shown to be involved in photorespiration, GLDPC was suggested to be involved in the maintenance of basal C_1 metabolism (Schulze et al. 2013). Promoter analysis showed that *GLDPA* was expressed only in bundle sheath cells in C_3 and C_4 *Flaveria* species, whereas *GLDPB* was expressed both in mesophyll and bundle sheath cells in C_3 species and became a pseudogene in C_4 *Flaveria* species (Schulze et al. 2013; Wiludda et al. 2012). In the C_3–C_4 intermediate species, the expression of *GLDPA* was upregulated, while that of *GLDPB* was downregulated, allowing C_2 photosynthesis to function at a high activity (Schulze et al. 2013). The bundle sheath cell-specific expression of the *GLDP* gene can be achieved by altering the *cis*-regulatory elements of the promoter region during evolution, as shown in *Arabidopsis thaliana*, where the deletion of a *cis*-regulatory module required for mesophyll cell-specific expression, called the

"M-box," resulted in bundle sheath cell-specific expression of the *GLDP* genes (Adwy et al. 2015).

The next step was how the C_4 cycle was developed in the C_3–C_4 intermediate stage toward the establishment of C_4 photosynthesis. The genus *Flaveria* contains a number of C_3–C_4 intermediate species classified as type II C_2 species that express C_4 cycle enzymes to some extent, as shown in Table 1, but these C_4 cycle enzymes do not contribute to the concentration of CO_2 (Ku et al. 1991; Monson et al. 1988). It has been suggested that these C_4 cycle enzymes are upregulated to rebalance nitrogen metabolism under C_2 photosynthesis (Mallmann et al. 2014; Schulze et al. 2016). Since the glycine decarboxylation reaction releases toxic ammonia that should be taken up by the bundle sheath chloroplasts, it creates an imbalance in nitrogen metabolism between mesophyll and bundle sheath chloroplasts. By using a computer simulation model, a malate/alanine shuttling between mesophyll and bundle sheath cells was predicted to be coupled with a glycine/serine shuttling (Mallmann et al. 2014). Operation of this metabolic pathway was supported by upregulation of alanine aminotransferase together with NADP-malic enzyme (NADP-ME) in C_3–C_4 intermediate species (Mallmann et al. 2014). However, C_4 cycle enzymes were expressed in both mesophyll and bundle sheath cells in C_3–C_4 intermediate species (Moore 1988; Taniguchi et al. 2021), which indicates that the produced C_4 compounds could be metabolized within a cell without transfer to adjacent cells (Fig. 3). While equal distribution of the C_4 enzyme between mesophyll and bundle sheath cells was observed in *F. floridana*, weak cell selective distribution of the C_4 cycle enzyme was observed in *F. ramosissima* (Table 1) (Taniguchi et al. 2021). The selective cell distribution became stronger in C_4-like *F. brownii* (Table 1) (Taniguchi et al. 2021). In this species, the level of PEPC expression does not reach the level of that in C_4 species (0.3 times that of C_4 species, Table 1), but functional operation of the C_4 cycle that contributes to CO_2 concentration in bundle sheath cells was reported (Cheng et al. 1988; Monson et al. 1988). This evidence shows that cell-specific expression was gradually gained during the C_3–C_4 intermediate stage and elevated flux of the C_4 cycle between mesophyll and bundle sheath cells. The following scenarios were possible: (1) in the early C_3–C_4 intermediate stage, multiple metabolic pathways, including 2-oxoglutarate/glutamate, pyruvate/alanine and malate/aspartate shuttles, may have been used to balance nitrogen metabolism under C_2 photosynthesis, as predicted by computer simulation (Mallmann et al. 2014). C_4 cycle enzymes and N- and C-balancing enzymes, such as alanine-aminotransferase and aspartate-aminotransferase, were upregulated in response to metabolic imbalance but in a noncell selective manner; therefore, the flux of the two-celled C_4 cycle must have been very low (Fig. 3A). (2) Cell-selective expression of C_4 cycle enzymes was gradually acquired to correct the metabolic imbalance more efficiently, and the resulting increase in the flux of the two-celled C_4 cycle may have functioned to concentrate CO_2. Subsequent suppression of RuBisCO expression in mesophyll cells may have reduced RuBisCO oxygenase activity and replaced the C_2 cycle with the C_4 cycle at a C_4-like stage (Fig. 3B). Suppression of RuBisCO expression in mesophyll cells was not observed in *F. ramosissima* but in *F. brownii*, indicating that it was induced after the establishment of a high flux of the two-celled C_4 cycle. (3) Finally, C_4 photosynthesis was established by complete suppression of RuBisCO expression in mesophyll cells (Fig. 3C).

Optimization of the photochemical reaction and energy supply by reduction of photosystem II (PSII) activity and upregulation of cyclic electron transport

The electron transport system in chloroplasts was modified to optimize the energy supply during C_4 evolution. Since in the linear electron transport from water to NADPH, the number of protons transferred with an electron transfer is fixed, the ratio of ATP to NADPH production was estimated to be 9/7 (Allen 2003). C_4 photosynthesis requires more ATP to drive the C_4 cycle so that the ratio of ATP/NADPH demand in chloroplasts increases with the development of the C_4 cycle during C_4 evolution. In NAD-malic enzyme (NAD-ME)-type C_4 photosynthesis, ATP/NADPH demand increased in mesophyll cells, whereas in NADP-ME-type C_4 photosynthesis, it increased in bundle sheath cells because reducing power was shuttled as malate from mesophyll to bundle sheath cells (Kanai and Edwards 1999). A part of the C_3 cycle from phosphorylation of 3-PGA and subsequent reduction to production of triose phosphate is known to occur in mesophyll cells in C_4 species (Fig. 3C) (Kanai and Edwards 1999). This metabolic pathway is important in allocating energy requirements in mesophyll chloroplasts but is not likely to be able to compensate for imbalanced ATP/NADPH demand between mesophyll and bundle sheath cells (Kanai and Edwards 1999; Munekage and Taniguchi 2016).

Cyclic electron transport (CET) around photosystem I can generate proton motive force driving ATP synthesis without the production of NADPH by recycling electrons from ferredoxin to plastoquinone (Munekage 2016; Yamori and Shikanai 2016). There are two pathways of cyclic electron transport: the PGR5-PGRL1-dependent pathway and the NDH complex-dependent pathway (DalCorso et al. 2008; Munekage et al. 2002; Peltier et al. 2016). The abundances of NDH subunits were higher corresponding to the elevation of ATP demand in bundle sheath chloroplasts in NADP-ME type C_4 species or in mesophyll chloroplasts in NAD-ME type C_4 species (Kubicki et al. 1994; Majeran et al. 2008;

Takabayashi et al. 2005), indicating that NDH-dependent pathways were used to supply the ATP required for C_4 photosynthesis. Interestingly, the NDH subunit was elevated in the C_3–C_4 intermediate *F. ramosissima* and C_4-like *F. brownii*, correlating with enhanced CET activity inferred from P700 oxidation kinetics (Nakamura et al. 2013) (Table 1). In C_3 photosynthesis, ATP/NADPH demand was estimated to be 1.55 when photorespiration/photosynthesis occurred at 1/4 (Osmond 1981). In C_3–C_4 intermediate species, if glycine/serine shuttling was taken into account, ATP/NADPH demand was only slightly increased to 1.57 in mesophyll cells by a phosphorylation step of glycerate to produce 3-PGA and regeneration steps of RuBP from 3-PGAs that were also produced by RuBisCO oxygenation; whereas NH_3 uptake by glutamate synthase (GS) and glutamine-oxoglutarate aminotransferase (GOGAT), which consumed one molecule of ATP and 2 electrons counted as one molecule of NADPH, decreased the ATP/NADPH demand in bundle sheath cells, indicating that glycine/serine shuttling did not influence the ATP/NADPH demand in chloroplasts. However, if the C_4 cycle was coupled with the glycine/serine shuttle, the total ATP/NADPH demand was increased to 1.65. If reducing power was shuttled as malate from mesophyll to bundle sheaths where it was decarboxylated by NADP-ME, it elevated ATP/NADPH demand in bundle sheath chloroplasts. CET activity was only slightly elevated in C_3–C_4 intermediate *F. floridana* but was substantially elevated in C_3–C_4 intermediate *F. ramosissima* and C_4-like *F. brownii*, corresponding to the phenotypes where cell-selective distribution of the C_4 enzyme was observed (Table 1) (Nakamura et al. 2013). These results suggest that the acquisition of cell-selective expression of the C_4 enzyme increased the flux of the C_4 cycle, consequently increasing the demand for ATP/NADPH and that CET activity, especially NDH-dependent CET activity, was upregulated to fine-tune the ATP supply in the C_3–C_4 intermediate stage.

In C_4 species in the genus *Flaveria*, ATP/NADPH demand was estimated to be 1.9 and 5 in mesophyll and bundle sheath cells, respectively, where leakage of CO_2 from the bundle sheath to mesophyll cells is neglected (Munekage and Taniguchi 2016). Corresponding to the elevated ATP/NADPH demand, CET activity was further upregulated in C_4 species (Table 1). In these species, not only malate but also aspartate is transported to the bundle sheath cells, where it is converted back to oxaloacetate and then reduced to malate, which is decarboxylated by NADP-ME; therefore, the PSII activity of bundle sheath chloroplasts remains up to 20% of that of mesophyll chloroplasts to produce NADPH via linear electron transport (Hofer et al. 1992; Meister et al. 1996). The grana index correlated well with PSII activity and was relatively higher in bundle sheath chloroplasts in *Flaveria* C_4 species (15–19%) than in those in *Zea mays* and *Sorghum bicolor*, which have little PSII activity (Table 1) (Andersen et al. 1972; Nakamura et al. 2013; Woo et al. 1970). Notably, bundle sheath chloroplasts in C_4-like *F. brownii* showed a high grana index (50%) similar to those observed in mesophyll chloroplasts (Holaday et al. 1984; Nakamura et al. 2013). Because C_4-like *F. palmeri* and C_4 *F. bidentis* showed much slower P700 oxidation kinetics than C_4-like *F. brownii* (Table 1), the nonstacked thylakoid membrane structure and the suppression of PSII may contribute to the elevation of CET activity. These results also suggest that the optimization of electron transport by suppression of PSII was induced at a late stage of C_4 evolution.

Conclusions

C_4 evolution proceeded through various C_3–C_4 intermediate stages, where a photorespiration-dependent CO_2 enrichment system (C_2 photosynthesis) was first acquired, which may have led to the acquisition of two-celled C_4 cycles. The genus *Flaveria* is one of the most useful models to study C_4 evolution since it contains a large number of C_3–C_4 intermediate and C_4-like species that are closely related to C_4 species. The intermediate features between C_3 and C_4 displayed by these species indicate that most key C_4 traits, including localization of GDCs in mitochondria of bundle sheath cells, upregulation and cell-selective regulation of C_4 cycle-related genes, suppression of RuBisCO in mesophyll cells, upregulation of cyclic electron transport activity and suppression of PSII activity in bundle sheath chloroplasts, were all gradually acquired during C_4 evolution. The fact that these traits were acquired at different times suggests that a change that is dominant for survival triggers the next dominant change by natural selection, optimizing the system by modifying the balance of metabolism, gene expression, and energy supply.

Currently, the direct introduction of the C_4 cycle into C_3 plants is being attempted as a way to engineer C_4 photosynthesis. However, in these transformants, it was reported that bundle sheath chloroplasts were not well developed, resulting in insufficient expression of bundle sheath chloroplast proteins and that the C_4 cycle did not function well and there was an imbalance in metabolism and reducing power (Ermakova et al. 2021; Lin et al. 2020; Taniguchi et al. 2008). Since C_4 photosynthesis is a well-optimized and sophisticated system, it is necessary to modify the support system simultaneously with the introduction of the C_4 cycle. The evolutionary process of C_4 photosynthesis shows a trait change toward C_4 based on genomic changes. Using technologies such as genome editing to introduce genome modifications that mimic the evolution of C_4 photosynthesis may enable the engineering of C_4 photosynthesis in the future.

Author contributions YNM wrote the manuscript. YYT performed the anatomical analysis and measurements of CO_2 compensation points and O_2 inhibition of photosynthetic activity.

Funding This work was supported by JSPS KAKENHI (Grant Nos. 17K07456, 16H06557 and 21K05520) from the Japan Society for the Promotion of Science.

Declarations

Conflict of interest The authors declare there is no conflict of interest.

References

Adwy W, Laxa M, Peterhansel C (2015) A simple mechanism for the establishment of C_2-specific gene expression in Brassicaceae. Plant J 84:1231–1238

Allen JF (2003) Cyclic, pseudocyclic and noncyclic photophosphorylation: new links in the chain. Trends Plant Sci 8:15–19

Andersen KS, Bain JM, Bishop DG, Smillie RM (1972) Photosystem II activity in agranal bundle sheath chloroplasts from *Zea mays*. Plant Physiol 49:461–466

Araus JL, Brown RH, Bouton JH, Serret MD (1990) Leaf anatomical characteristics in *Flaveria trinervia* (C_4), *Flaveria brownii* (C_4-like) and their F1 hybrid. Photosynth Res 26:49–57

Bauwe H (2011) Chapter 6 photorespiration: the bridge to C_4 photosynthesis. In: Raghavendra AS, Sage RF (eds) C_4 photosynthesis and related CO_2 concentrating mechanisms. Springer, Dordrecht, pp 81–108

Brown RH, Hattersley PW (1989) Leaf anatomy of C_3–C_4 species as related to evolution of C_4 photosynthesis. Plant Physiol 91:1543–1550

Cheng SH, Moore BD, Edwards GE, Ku MS (1988) Photosynthesis in *Flaveria brownii*, a C_4-like species: leaf anatomy, characteristics of CO_2 exchange, compartmentation of photosynthetic enzymes, and metabolism of CO_2. Plant Physiol 87:867–873

Christin PA, Osborne CP, Sage RF, Arakaki M, Edwards EJ (2011) C_4 eudicots are not younger than C_4 monocots. J Exp Bot 62:3171–3181

DalCorso G, Pesaresi P, Masiero S, Aseeva E, Schunemann D, Finazzi G, Joliot P, Barbato R, Leister D (2008) A complex containing PGRL1 and PGR5 is involved in the switch between linear and cyclic electron flow in Arabidopsis. Cell 132:273–285

Edwards GE, Voznesenskaya EV (2011) Chapter 4 C_4 photosynthesis: Kranz forms and single-cell C_4 in terrestrial plants. In: Raghavendra AS, Sage RF (eds) C_4 photosynthesis and related CO_2 concentrating mechanisms. Springer, Dordrecht, pp 29–61

Edwards EJ, Osborne CP, Stromberg CA, Smith SA, Consortium CG, Bond WJ, Christin PA, Cousins AB, Duvall MR, Fox DL, Freckleton RP, Ghannoum O, Hartwell J, Huang Y, Janis CM, Keeley JE, Kellogg EA, Knapp AK, Leakey AD, Nelson DM, Saarela JM, Sage RF, Sala OE, Salamin N, Still CJ, Tipple B (2010) The origins of C_4 grasslands: integrating evolutionary and ecosystem science. Science 328:587–591

Ermakova M, Arrivault S, Giuliani R, Danila F, Alonso-Cantabrana H, Vlad D, Ishihara H, Feil R, Guenther M, Borghi GL, Covshoff S, Ludwig M, Cousins AB, Langdale JA, Kelly S, Lunn JE, Stitt M, von Caemmerer S, Furbank RT (2021) Installation of C_4 photosynthetic pathway enzymes in rice using a single construct. Plant Biotechnol J 19:575–588

Hall LN, Rossini L, Cribb L, Langdale JA (1998) GOLDEN 2: a novel transcriptional regulator of cellular differentiation in the maize leaf. Plant Cell 10:925–936

Hofer MU, Santore UJ, Westhoff P (1992) Differential accumulation of the 10-, 16- and 23-kDa peripheral components of the water-splitting complex of photosystem II in mesophyll and bundle-sheath chloroplasts of the dicotyledonous C_4 plant *Flaveria trinervia* (Spreng.) C. Mohr. Planta 186:304–312

Holaday AS, Lee KW, Chollet R (1984) C_3–C_4 intermediate species in the genus *Flaveria*: leaf anatomy, ultrastructure, and the effect of O_2 on the CO_2 compensation concentration. Planta 160:25–32

Huang CF, Yu CP, Wu YH, Lu MJ, Tu SL, Wu SH, Shiu SH, Ku MSB, Li WH (2017) Elevated auxin biosynthesis and transport underlie high vein density in C_4 leaves. Proc Natl Acad Sci USA 114:E6884–E6891

Jordan DB, Ogren WL (1984) The CO_2/O_2 specificity of ribulose 1,5-bisphosphate carboxylase/oxygenase: dependence on ribulosebisphosphate concentration, pH and temperature. Planta 161:308–313

Kanai R, Edwards G (1999) The biochemistry of C_4 photosynthesis. In: Sage R, Monson R (eds) C_4 plant biology. Academic Press, San Diego, pp 49–87

Ku MS, Wu J, Dai Z, Scott RA, Chu C, Edwards GE (1991) Photosynthetic and photorespiratory characteristics of *Flaveria* species. Plant Physiol 96:518–528

Kubicki A, Steinmüller K, Westhoff P (1994) Differential transcription of plastome-encoded genes in the mesophyll and bundle-sheath chloroplasts of the monocotyledonous NADP-malic enzyme-type C_4 plants maize and Sorghum. Plant Mol Biol 25:669–679

Lauterbach M, Schmidt H, Billakurthi K, Hankeln T, Westhoff P, Gowik U, Kadereit G (2017) De novo transcriptome assembly and comparison of C_3, C_3–C_4, and C_4 species of tribe Salsoleae (Chenopodiaceae). Front Plant Sci 8:1939

Lin H, Arrivault S, Coe RA, Karki S, Covshoff S, Bagunu E, Lunn JE, Stitt M, Furbank RT, Hibberd JM, Quick WP (2020) A partial C_4 photosynthetic biochemical pathway in rice. Front Plant Sci 11:564463

Linh NM, Verna C, Scarpella E (2018) Coordination of cell polarity and the patterning of leaf vein networks. Curr Opin Plant Biol 41:116–124

Long SP (1991) Modification of the response of photosynthetic productivity to rising temperature by atmospheric CO_2 concentrations: has its importance been underestimated? Plant Cell Environ 14:729–739

Lundgren MR, Osborne CP, Christin PA (2014) Deconstructing Kranz anatomy to understand C_4 evolution. J Exp Bot 65:3357–3369

Lyu MJ, Gowik U, Kelly S, Covshoff S, Mallmann J, Westhoff P, Hibberd JM, Stata M, Sage RF, Lu H, Wei X, Wong GK, Zhu XG (2015) RNA-Seq based phylogeny recapitulates previous phylogeny of the genus *Flaveria* (Asteraceae) with some modifications. BMC Evol Biol 15:116

Majeran W, Zybailov B, Ytterberg AJ, Dunsmore J, Sun Q, van Wijk KJ (2008) Consequences of C_4 differentiation for chloroplast membrane proteomes in maize mesophyll and bundle sheath cells. Mol Cell Proteomics MCP 7:1609–1638

Mallmann J, Heckmann D, Brautigam A, Lercher MJ, Weber AP, Westhoff P, Gowik U (2014) The role of photorespiration during the evolution of C_4 photosynthesis in the genus *Flaveria*. Elife 3:e02478

McKown AD, Dengler NG (2007) Key innovations in the evolution of Kranz anatomy and C_4 vein pattern in *Flaveria* (Asteraceae). Am J Bot 94:382–399

McKown AD, Dengler NG (2009) Shifts in leaf vein density through accelerated vein formation in C_4 *Flaveria* (Asteraceae). Ann Bot 104:1085–1098

McKown AD, Moncalvo JM, Dengler NG (2005) Phylogeny of *Flaveria* (Asteraceae) and inference of C_4 photosynthesis evolution. Am J Bot 92:1911–1928

Meister M, Agostino A, Hatch MD (1996) The roles of malate and aspartate in C_4 photosynthetic metabolism of *Flaveria bidentis* (L.). Planta 199:262–269

Monson RK, Teeri JA, Ku MS, Gurevitch J, Mets LJ, Dudley S (1988) Carbon-isotope discrimination by leaves of *Flaveria* species exhibiting different amounts of C_3-and C_4-cycle co-function. Planta 174:145–151

Moore BD, Monson RK, Ku MSB, Edwards GE (1988) Activities of principal photosynthetic and photorespiratory enzymes in leaf mesophyll and bundle sheath protoplasts from the C_3–C_4 intermediate *Flaveria ramosissima*. Plant Cell Physiol 29:999–1006

Munekage YN (2016) Light harvesting and chloroplast electron transport in NADP-malic enzyme type C_4 plants. Curr Opin Plant Biol 31:9–15

Munekage YN, Taniguchi YY (2016) Promotion of cyclic electron transport around photosystem I with the development of C_4 photosynthesis. Plant Cell Physiol 57:897–903

Munekage Y, Hojo M, Meurer J, Endo T, Tasaka M, Shikanai T (2002) PGR5 is involved in cyclic electron flow around photosystem I and is essential for photoprotection in Arabidopsis. Cell 110:361–371

Munekage YN, Eymery F, Rumeau D, Cuine S, Oguri M, Nakamura N, Yokota A, Genty B, Peltier G (2010) Elevated expression of PGR5 and NDH-H in bundle sheath chloroplasts in C_4 *Flaveria* species. Plant Cell Physiol 51:664–668

Nakamura N, Iwano M, Havaux M, Yokota A, Munekage YN (2013) Promotion of cyclic electron transport around photosystem I during the evolution of NADP-malic enzyme-type C_4 photosynthesis in the genus *Flaveria*. New Phytol 199:832–842

Osmond CB (1981) Photorespiration and photoinhibition: some implications for the energetics of photosynthesis. Biochim Biophys Acta (BBA) Rev Bioenerg 639:77–98

Peltier G, Aro EM, Shikanai T (2016) NDH-1 and NDH-2 plastoquinone reductases in oxygenic photosynthesis. Annu Rev Plant Biol 67:55–80

Powell AM (1978) Systematics of *Flaveria* (Flaveriinae–Asteraceae). Ann Mo Bot Gard 65:590–636

Rossini L, Cribb L, Martin DJ, Langdale JA (2001) The maize golden2 gene defines a novel class of transcriptional regulators in plants. Plant Cell 13:1231–1244

Sage RF, Sage TL, Kocacinar F (2012) Photorespiration and the evolution of C_4 photosynthesis. Annu Rev Plant Biol 63:19–47

Sage TL, Busch FA, Johnson DC, Friesen PC, Stinson CR, Stata M, Sultmanis S, Rahman BA, Rawsthorne S, Sage RF (2013) Initial events during the evolution of C_4 photosynthesis in C_3 species of *Flaveria*. Plant Physiol 163:1266–1276

Sage RF, Khoshravesh R, Sage TL (2014) From proto-Kranz to C_4 Kranz: building the bridge to C_4 photosynthesis. J Exp Bot 65:3341–3356

Sage RF, Monson RK, Ehleringer JR, Adachi S, Pearcy RW (2018) Some like it hot: the physiological ecology of C_4 plant evolution. Oecologia 187:941–966

Schulze S, Mallmann J, Burscheidt J, Koczor M, Streubel M, Bauwe H, Gowik U, Westhoff P (2013) Evolution of C_4 photosynthesis in the genus *Flaveria*: establishment of a photorespiratory CO_2 pump. Plant Cell 25:2522–2535

Schulze S, Westhoff P, Gowik U (2016) Glycine decarboxylase in C_3, C_4 and C_3–C_4 intermediate species. Curr Opin Plant Biol 31:29–35

Sedelnikova OV, Hughes TE, Langdale JA (2018) Understanding the genetic basis of C_4 Kranz anatomy with a view to engineering C_3 crops. Annu Rev Genet 52:249–270

Takabayashi A, Kishine M, Asada K, Endo T, Sato F (2005) Differential use of two cyclic electron flows around photosystem I for driving CO_2-concentration mechanism in C_4 photosynthesis. Proc Natl Acad Sci USA 102:16898–16903

Taniguchi Y, Ohkawa H, Masumoto C, Fukuda T, Tamai T, Lee K, Sudoh S, Tsuchida H, Sasaki H, Fukayama H, Miyao M (2008) Overproduction of C_4 photosynthetic enzymes in transgenic rice plants: an approach to introduce the C_4-like photosynthetic pathway into rice. J Exp Bot 59:1799–1809

Taniguchi YY, Gowik U, Kinoshita Y, Kishizaki R, Ono N, Yokota A, Westhoff P, Munekage YN (2021) Dynamic changes of genome sizes and gradual gain of cell-specific distribution of C_4 enzymes during C_4 evolution in genus *Flaveria*. Plant Genome 14:e20095

Voznesenskaya EV, Koteyeva NK, Edwards GE, Ocampo G (2017) Unique photosynthetic phenotypes in Portulaca (Portulacaceae): C_3–C_4 intermediates and NAD-ME C_4 species with Pilosoid-type Kranz anatomy. J Exp Bot 68:225–239

Wang P, Fouracre J, Kelly S, Karki S, Gowik U, Aubry S, Shaw MK, Westhoff P, Slamet-Loedin IH, Quick WP, Hibberd JM, Langdale JA (2013) Evolution of GOLDEN2-LIKE gene function in C_3 and C_4 plants. Planta 237:481–495

Wang P, Khoshravesh R, Karki S, Tapia R, Balahadia CP, Bandyopadhyay A, Quick WP, Furbank R, Sage TL, Langdale JA (2017) Re-creation of a key step in the evolutionary switch from C_3 to C_4 leaf anatomy. Curr Biol 27:3278-3287.e6

Williams BP, Johnston IG, Covshoff S, Hibberd JM (2013) Phenotypic landscape inference reveals multiple evolutionary paths to C_4 photosynthesis. Elife 2:e00961

Wiludda C, Schulze S, Gowik U, Engelmann S, Koczor M, Streubel M, Bauwe H, Westhoff P (2012) Regulation of the photorespiratory GLDPA gene in C_4 *Flaveria*: an intricate interplay of transcriptional and posttranscriptional processes. Plant Cell 24:137–151

Woo KC, Anderson JM, Boardman NK, Downton WJ, Osmond CB, Thorne SW (1970) Deficient photosystem II in agranal bundle sheath chloroplasts of C_4 plants. Proc Natl Acad Sci USA 67:18–25

Yamori W, Shikanai T (2016) Physiological functions of cyclic electron transport around photosystem I in sustaining photosynthesis and plant growth. Annu Rev Plant Biol 67:81–106

Yorimitsu Y, Kadosono A, Hatakeyama Y, Yabiku T, Ueno O (2019) Transition from C_3 to proto-Kranz to C_3–C_4 intermediate type in the genus *Chenopodium* (Chenopodiaceae). J Plant Res 132:839–855